

## Photon Generation by Joule Heating in Metal Films

N. Perrin and H. Budd

*Groupe de Physique des Solides de l'École Normale Supérieure,\* Université de Paris VII, Paris, France*

(Received 13 March 1972)

We calculate the evolution of the coupled electron-phonon system in a metal film subjected to an electric field. The detailed form of the phonon distribution is presented, and is shown to deviate significantly from a Bose distribution.

Recently there has been considerable experimental and theoretical work on heat-pulse propagation in solids.<sup>1-4</sup> In a typical heat-pulse experiment one generates high-frequency phonons, which then impinge on some target and are subsequently detected. The most commonly employed method for generating such phonons is that of passing an electrical current through a metallic film, evaporated on one end of the sample being studied.

In this Letter we shall consider the details of this phonon-generation scheme. One obviously requires a fairly decent knowledge of the generated phonon distribution, in order to deduce useful information relevant to the system (target) being studied. The simplest, and most commonly employed, approximation is to assume that the metallic film can be characterized by a temperature  $T_e$ ,<sup>1,2</sup> which may be time dependent.<sup>4</sup> The latter is then calculated from an appropriate energy-conservation equation. Implicit in such a treatment is the assumption that the electrons and phonons are essentially in equilibrium with one another.

We believe this model to be inappropriate for the following reason. A phonon of wave vector  $\vec{q}$  is characterized by a relaxation time<sup>5</sup>  $\tau_{ep} \propto q^{-1}$  due to its interaction with the conduction electrons in the metal. On the other hand, the time required for the phonon distribution to thermalize to the substrate (sample) temperature is of the order of  $\tau_b \approx \eta d/c$ , where  $d$  is the film thickness,  $c$  an average sound velocity, and  $\eta$  a factor which measures the acoustic mismatch at the metal-sample interface. We note that  $\eta$  is of the order of 1 for a metal-solid contact, although it can be quite large for a metal-liquid-helium interface. It is therefore clear that sufficiently long-wavelength ( $\tau_{ep} \gg \tau_b$ ) phonons will remain essentially in equilibrium with the substrate. For thin films,  $\tau_b$  is relatively short and one expects a large portion of the phonon distribution not to be in equilibrium with the electrons.

A detailed analysis of this problem is clearly

impossible since it would require solving for the coupled time- and space-dependent electron and phonon distributions, with due regard to the boundary conditions at the interface. The essential point we wish to emphasize is that as far as the phonons are concerned, their most effective interaction is with the heat bath (substrate).

In order to formulate a tractable model we introduce the following simplifications: (1) The phonon distribution  $N_q$  relaxes towards the substrate temperature with the time constant  $\tau_b$ ; (2) the electron distribution is characterized by a Fermi-Dirac distribution at temperature  $T_e(t)$ , the latter being determined by an energy balance equation. The evolution of the phonon distribution  $N_q$  is then given by

$$\frac{\partial N_q}{\partial t} = \frac{\bar{N}_q(T_e) - N_q}{\tau_{ep}} + \frac{\bar{N}_q(T_0) - N_q}{\tau_b}, \quad (1)$$

where  $\bar{N}_q(T)$  is the Planck distribution at  $T$  and

$$\tau_{ep}^{-1} = E_1^2 m^2 \omega_q / 2\hbar^3 \pi \rho u. \quad (2)$$

In Eqs. (1) and (2),  $E_1$  is the deformation potential constant,  $m$  is the electron mass,  $u$  is the longitudinal sound velocity,  $\rho$  is the mass density of the metal, and  $\omega_q$  is the frequency of phonons of wave vector  $\vec{q}$ .

The first term in Eq. (1) is readily derived for phonons interacting with a degenerate electron gas at temperature  $T_e$ , and expresses the tendency for the phonons to reach equilibrium with the electrons. The slight anisotropy of the electron distribution, due to the applied electric field, has been neglected.

The second term is our phenomenological representation of the relaxation of the phonon distribution to a Bose distribution at the ambient temperature. This formulation considerably simplifies the mathematical analysis and retains the essential physics of the problem. The detailed form of the electron distribution is extremely difficult to calculate, and we have adopted the usual Fermi-Dirac approximation. This clearly introduces no qualitative error in the present

context, and without this simplification no further progress is possible. In any event, we go one step further than the usual model in which both the forms of the electron and phonon distributions are taken *a priori*.

The evolution of the electron distribution is determined by the following energy-balance equation:

$$C_e \frac{\partial T_e}{\partial t} = \sigma E^2 - \sum_{\vec{q}} \hbar \omega_{\vec{q}} \frac{\bar{N}_{\vec{q}}(T_e) - N_{\vec{q}}}{\tau_{ep}}, \quad (3)$$

where  $C_e$  is the electronic specific heat, and  $\sigma$  the electrical conductivity. In typical evaporated films,  $\sigma$  is relatively temperature independent at low temperatures, since the residual resistivities  $\rho_R$  are high. We shall take account of this

slight variation by a simple generalization of the usual treatment of electrical resistivity. We calculate the rate of momentum transfer from a displaced electron distribution  $f_0(\vec{V} - \vec{V}_d)$  to the phonons, where  $f_0$  is the Fermi-Dirac distribution. We obtain

$$\sum_{\vec{q}} \hbar \vec{q} \left( \frac{\partial N_{\vec{q}}}{\partial t} \right)_{ep} = \sum_{\vec{q}} \hbar \vec{q} \frac{\bar{N}_{\vec{q}}^*(T_e) - N_{\vec{q}}}{\tau_{ep}^*}, \quad (4)$$

where the starred quantities are the same as in Eq. (1), except evaluated at the Doppler-shifted phonon frequency  $\omega_{\vec{q}} - \vec{q} \cdot \vec{V}_d$ . Linearizing in  $\vec{V}_d$ , and equating this momentum-transfer rate to the applied force  $e\vec{E}$ , yields the drift velocity and hence the phonon contribution to the electrical resistivity,  $\rho_{ph}$ . For an isotropic, but otherwise arbitrary phonon distribution  $N_{\vec{q}}$ , we obtain

$$\rho_{ph} = \frac{m}{ne^2\tau_a}, \quad \frac{1}{\tau_a} = \frac{1}{k_F^3} \frac{mE_1^2}{4\pi\rho u\hbar^2} \left\{ - \int_0^{q_D} q^5 \frac{\partial \bar{N}_{\vec{q}}(T_e)}{\partial q} dq + \int_0^{q_D} q^4 [N_{\vec{q}} - \bar{N}_{\vec{q}}(T_e)] dq \right\}, \quad (5)$$

where  $n$  is the electron density,  $k_F$  is the Fermi wave number, and  $q_D$  is the Debye wave number. The presence of the second term on the right-hand side of Eq. (5) is due to the fact that the phonons are not in equilibrium with the electrons. This term vanishes for the equilibrium case,  $N_{\vec{q}} = \bar{N}_{\vec{q}}(T_0) = \bar{N}_{\vec{q}}(T_e)$ , and Eq. (5) reduces to the usual expression, derived from Koehler's variational theorem.<sup>6</sup> The total resistivity is therefore approximately given by

$$\rho = \rho_R + \rho_{ph}.$$

In any case, this slight variation of the resistivity is of little importance for the determination of the evolution of the electron-phonon system. The solution of the coupled Eqs. (1) and (3) for a typical monovalent metal (Au:  $n = 6 \times 10^{28} \text{ m}^{-3}$ ,  $\rho_R = 5 \times 10^{-8} \Omega \text{ m}$ ,  $u = 5 \times 10^3 \text{ m sec}^{-1}$ , film thickness  $d = 10^3 \text{ \AA}$ ) is carried out on an IBM 360.75.

A small time interval  $\Delta t$  is considered, during which  $N_{\vec{q}}$  and  $T_e$  undergo small variations determined by Eqs. (1) and (3). This yields  $N_{\vec{q}}$  and  $T_e$  at time  $t + \Delta t$ , from which one deduces the variations in the subsequent time interval, etc.

Typical results are shown in Figs. 1-3. The evolution of the energy-density spectrum  $q^3 N_{\vec{q}}$  is shown in Fig. 1. We note that with respect to the equilibrium distribution (lowest curve), most of the heating of the phonon distribution occurs for the high-frequency modes, the low-frequency modes remaining essentially at their equilibrium values. The upper curve, corresponding to roughly six transit times, is essentially the steady-state phonon distribution. In Fig. 2 is shown the

steady-state energy density spectrum of the phonon distribution calculated for  $E = 16 \text{ V cm}^{-1}$ , and the usual Bose approximation; the upper curve corresponds to a Bose distribution having the same total energy as the calculated distribution. It grossly overestimates the energy density in the low-frequency modes, and consequently is a very poor representation of the phonon distribu-

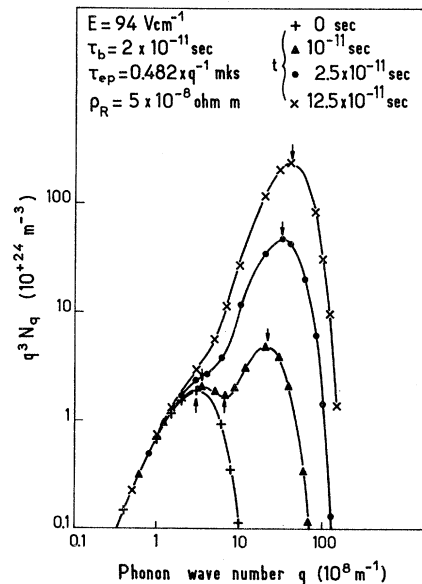


FIG. 1. Energy-density spectrum  $q^3 N_{\vec{q}}$  versus phonon wave number at different times. The curve at  $t = 0 \text{ sec}$  is the thermal equilibrium energy-density spectrum  $q^3 \bar{N}_{\vec{q}}(T_0 = 4.2^\circ \text{K})$ . The upper curve represents the steady state.

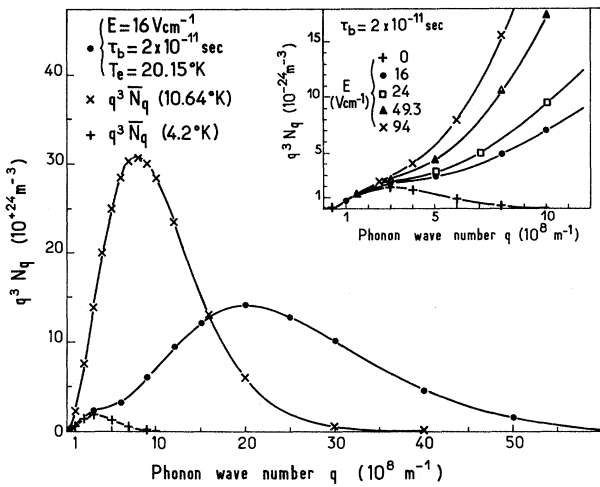


FIG. 2. Steady-state energy-density spectrum  $q^3 N_q$  versus phonon wave number. A comparison is made between the calculated distribution  $N_q$  for  $E = 16 \text{ V cm}^{-1}$  and a Bose distribution having the same energy. The curves in the inset correspond to different electric fields. The energy-density spectrum of the equilibrium Bose distribution (at 4.2°K) is shown for comparison.

tion. We also present, in the inset, the field dependence of the low-frequency portion of the steady-state energy density spectrum. Here again we see that the low-frequency modes are relatively unperturbed, while the high-frequency modes are extremely hot compared to the equilibrium distribution.

In order to have a simple representation of the difference between the Bose distribution and the steady-state one, we define the phonon temperature  $T_p(q)$  in each mode by

$$N_q \equiv \{\exp[\hbar\omega(q)/k_B T_p(q)] - 1\}^{-1}.$$

The phonon temperature  $T_p(q)$  is shown in Fig. 3 along with the electron temperature at the corresponding instants. Here one sees clearly that the high-frequency phonons are characterized by a temperature close to, but slightly below, the electron temperature. In the steady state their temperature is within roughly 5–10% of the electron temperature. The lower-frequency phonons, on the other hand, have considerably lower temperatures since their interaction with the electrons is weak,  $\tau_{ep}^{-1} \propto \omega_q$ . A Bose approximation

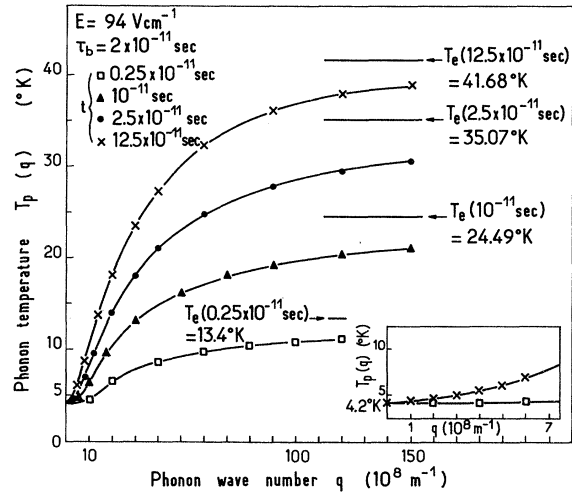


FIG. 3. Phonon temperature  $T_p(q)$  versus wave number  $q$  at different times, and the corresponding electron temperature.

for the phonon distribution, i.e.,  $T_p(q)$  independent of  $q$ , is clearly impossible.

In summary then, the coupled electron-phonon system is characterized by a distinctly non-Bose-type distribution function. The detailed form depends on the film thickness and the acoustic mismatch at the interface, through  $\tau_b$ , and on the intensity of the electron-phonon interaction. A more realistic calculation of the coupled system requires a solution of the appropriate equations, including the spatial variation of the distribution functions, but will probably yield the same qualitative results presented here.

\*Laboratory associated with Centre National de la Recherche Scientifique.

<sup>1</sup>R. J. Von Gutfeld, *Physical Acoustics* (Academic, New York, 1968), Vol. V.

<sup>2</sup>V. Narayanamurti, *Phys. Lett.* **30A**, 521 (1969).

<sup>3</sup>J. P. Maneval, A. Zylbersztein, and D. Huet, *Phys. Rev. Lett.* **27**, 1375 (1971).

<sup>4</sup>P. C. Kwok, *Phys. Rev.* **175**, 3 (1968).

<sup>5</sup>J. M. Ziman, *Phil. Mag.* **1**, 191 (1956), and corrigendum.

<sup>6</sup>J. M. Ziman, *Electrons and Phonons* (Clarendon Press, Oxford, England, 1962).